New Local Geoid Model for Northern Greece

V.D. ANDRITSANOS, A. FOTIOU, C. PIKRIDAS, D. ROSSIKOPOULOS and I.N. TZIAVOS, Greece and G. FOTOPOULOS, Canada

Key words: GPS-leveling, geoid heights, high resolution DTM, GPS-benchmark distribution

SUMMARY

In this paper a new local geoid model for the northern part of Greece is presented as part of an ongoing effort to improve the geoid heights in this area. The gravimetric geoid heights are derived using the latest gravity data available in the $40.3 < \varphi < 41$, $22.5 < \lambda < 24.3$ coverage area as well as a $1km \times 1km$ digital terrain model (DTM). Comparisons using a newly available high resolution $90m \times 90m$ DTM grid are also performed in order to draw conclusions on the adequacy of this higher resolution DTM in the area of interest. The gravimetrically derived geoid heights are used in a common adjustment with more than 140 GPS/leveling benchmark values to compute parameters for various transformation models. Problems arising from the geographical distribution of clusters of GPS/leveling in the surrounding area are discussed providing an account of the most suitable location for proposed benchmark sites. The final solution is aimed for levelling by GPS in and surrounding Thessaloniki, which is indispensable for a variety of engineering surveying applications.

New Local Geoid Model for Northern Greece

V.D. ANDRITSANOS, A. FOTIOU, C. PIKRIDAS, D. ROSSIKOPOULOS and I.N. TZIAVOS, Greece and G. FOTOPOULOS, Canada

1. INTRODUCTION

The purpose of this paper is to present the latest results for the new local geoid model in the northern part of Greece. This is a continuation of a series of studies conducted using various computation methods and available data sources (see Andritsanos et al., 1999 and Andritsanos et al., 2000). In this particular study, four different geoid model solutions were computed and tested in order to determine the best solution for leveling by GPS in the greater Thessaloniki area. The four solution types and their corresponding input data are shown in Figure 1. Models A and B represent the gravimetric quasi-geoid solutions computed using validated gravity data and the GINA and SRTM digital terrain models (DTM), respectively. Models C and D represent the combined geoid model solutions using the same validated gravity data, GPS/leveling benchmark data and the GINA and SRTM DTMs, respectively. The discussion begins with a description of the data used for each type of geoid model solution. This includes an important data validation step performed on the gravity database. Following the theoretical development and computation of each geoid model solution is provided. The analysis of results is shown as the discussion progresses. Possible improvements suggested for future surveys especially with regards of strategic densification of the existing GPS/leveling benchmark network in the area of interest is provided in the concluding remarks.

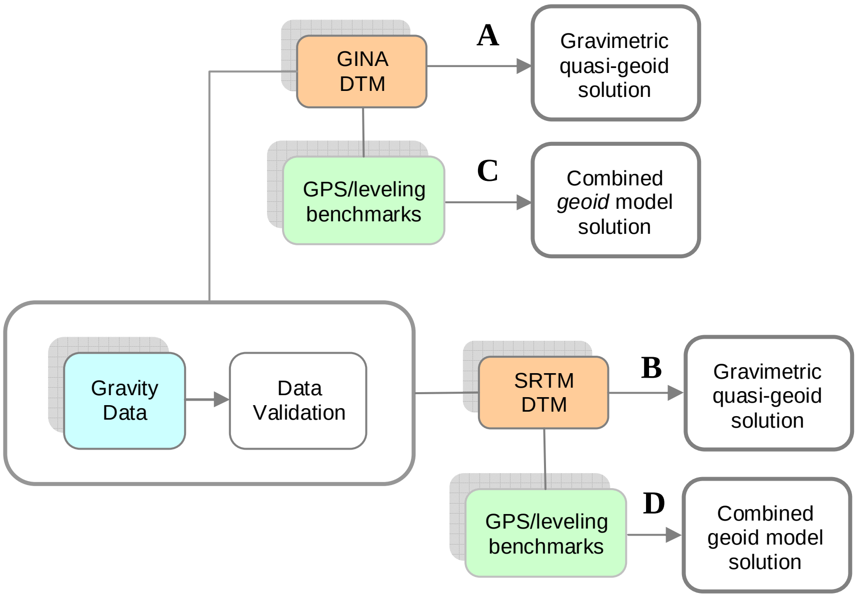

Figure 1: Overview of gravimetric quasi-geoid solutions (A and B) and combined geoid model solutions (C and D)

2. DESCRIPTION AND TREATMENT OF DATA

2.1 Gravity Data

The area for the geoid computation is located in the central Macedonia region of Greece. The boundaries of the geoid solution extend to $39.5 \le \varphi \le 42.5$ and $22 \le \lambda \le 24$. This is a very interesting area for a GPS/leveling test campaign due to the very high altitude variation between the mountains of central Greece and the depth of the Aegean Sea. Point free-air gravity anomalies for the continental part of Greece were used. These data are part of the database covering the Greek territory and are referred to IGSN71 using the gravity formula of 1980 for the normal gravity computation (Andritsanos et al., 1999). The horizontal datum is the global GRS80 ellipsoid. The height of the measurement is based on the vertical reference point of the Pireas port. Altimetry derived as well as map digitized free-air gravity anomalies were used in the sea area. The altimetric data are part of the KMS02 gravity database that was computed using inverse methods. The resolution of the altimetry-derived gravity anomalies is $3' \times 3'$ (Andersen and Knudsen, 1998). Contour free-air data were extracted from Morelli's maps of the Mediterranean Sea by digitization (Beherent et al., 1996). The locations of the free-air gravity anomalies used are pictured in Figure 2.

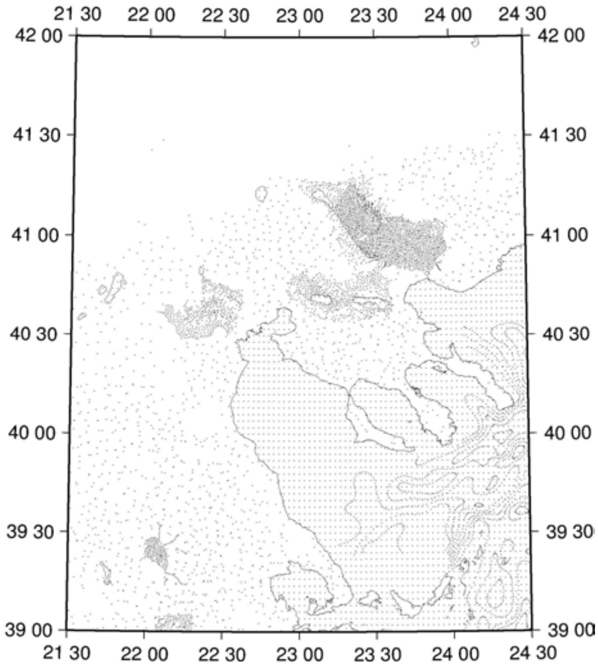

Figure 2: Free-air gravity anomaly data

2.2 Gravity Data Validation

The basic analysis and validation of the gravity databank is based on a gross-error detection visualization and collocation scheme. Taking into account that gravity field data are spatially correlated, gravity quantities of the same type and not far apart will be very similar.

Especially, after the removal of a) a highly expanded geopotential model and b) of the effect of the neighboring masses, the distribution of the data was very close to a normal distribution. A simple formation of the histogram of the data will therefore show the outliers. An effective check can also be done by 2D contouring the data (BGI, 1992). Thus, following this method, deep "holes" and steep spikes indicated suspicious observations. Since the smoothness of the field is the highest one after the removal of high and low frequency information, large discrepancies were identified as blunders.

Least squares collocation was also used to remove any existing outliers that could not remove during the preceding visual check (Tscherning, 1991). A gravity anomaly y was predicted from a set of values x, in neighboring points, spaced as evenly as possible in all directions according to the well-known collocation formula (Moritz, 1980)

$$\tilde{y} = C_y \overline{C}^{-1} x \tag{1}$$

where C_y is the vector of covariance between y and the x_i values, $\overline{C} = C + D$ is the sum of the covariance matrix of the x_i quantities and the variance-covariance matrix of the noise (error) associated with the quantities. An error estimate was also computed for the difference $|y - \tilde{y}|$ as

$$\sigma^2(y - \overline{y}) = C_o - C_y^T C^{-1} C_y \tag{2}$$

where C_o is the variance of the gravity values. A gross-error was then detected when

$$|y_{obs} - \tilde{y}| > k\sqrt{\sigma^2(y - \tilde{y}) + \sigma_y^2} \tag{3}$$

where k is a constant generally having the value 3 to 5 depending on the check strictness and σ_y^2 is the error variance of the observation y_{obs}. From the above equations it is obvious that gross-errors are most easily found if C_o is as small as possible. Thus it is obvious that the removal of the long and short wavelengths of the gravity field is necessary for the outlier detection to lead to rigorous results.

Upon the elimination of gross-errors using this technique, the total number of observations was then divided in two files with equal and homogeneously distributed data points. The data were reduced to the EGM96 geopotential model and RTM effects based on a 30″×30″ DTM for land and sea areas (see, next section) and an empirical covariance function was computed and fitted to an analytical model using the observations of the first data file. Using the parameters of this model, predictions at the locations of the points of the second file were estimated. Due to the unavailability of proper measurement error and the ambiguous quality of the observations an error of 5 mGals was assigned in each observation. The rejection criterion with a parameter k=3 was followed. This parameter in conjunction with the overestimated σ of the observations ensured the removal of the largest blunders. The gross-error detection procedure was repeated three times and stopped when no error can be determined. A total number of 317 points were rejected as suspicious gross-errors. The points removed represent a 3.5% of the total database. The statistics of the original gravity anomaly data as well as the final accepted free-air gravity anomalies are presented in Table 1.

Table 1: Gravity reductions and final accepted anomalies (mGal)

	# points	maximum	minimum	μ	σ
Δg_{orig}	9044	189.2	-80.8	26.6	30.0
$\Delta g_{FA-accepted}$	8727	189.2	-78.5	25.9	29.6

2.3 GPS/Leveling Benchmark Data

A total number of 100 GPS/leveling benchmarks and 32 triangulation pillars of the national horizontal geodetic network were measured in the test area. The GPS benchmarks belong to the National Vertical Reference System. An area of $80km \times 60km$ was covered. The measurements were performed using two sets of Leica dual-frequency receivers System 300 and 500. The processing of GPS data was performed using the Bernese GPS software, version 4.0 (Rothacher and Mervart, 1996) and Leica SKI-Pro version 2.5 for the shortest baselines. Precise ephemerides from CODE were used. Coordinates for our permanent station named TATM were computed in ITRF94 for epoch 1997.86. The station coordinates were determined from IGS stations NOTO and MATERA, using observations for one week. Global ionospheric models from CODE were also used for the ambiguity resolution process. All GPS benchmark coordinates were computed from the known reference station, using at least one-hour observations in order to define them in the same system at the specific epoch. Free as well as constrained network adjustments were performed for the final GPS benchmark coordinates. A more detailed presentation of the GPS data processing and a study of the solution repeatability is presented in Andritsanos et al. (1999). It should be noted that all baseline ambiguities were successfully fixed to their integer values. Figure 3 depicts the current locations of the GPS/leveling benchmark stations. It is quite evident that although the number of points is quite large for the given coverage area, the distribution is very poor with clusters gathered at various highly populated parts and fewer points in rougher terrain areas. Clearly this is a situation that needs to be improved and the issue will be addressed in section 5 as prospects for future work.

2.4 Digital Terrain Models

In order to investigate the effect of the terrain to the geoid computation, two different digital terrain models were used. The first one is the product of a research project of the University of Alaska and is denoted as the GINA DTM. The resolution of GINA DTM is $30'' \times 30''$ both in land and marine areas (see GINA, 2004 for more details.). The second DTM investigated for use is part of the newly available data of Satellite Radar Topography Mission (SRTM) which has a higher resolution, namely $3'' \times 3''$, but covers only continental areas and therefore lacks bathymetry data (see SRTM, 2003 for details). The statistics of each DTM are presented in Table 2.

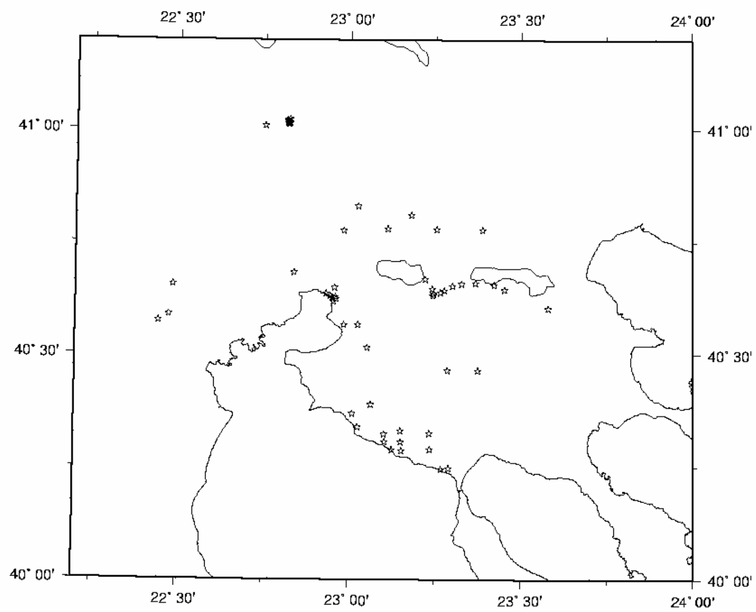

Figure 3: GPS/leveling benchmark network in northern Greece

Table 2: Statistics of the used DTMs (meters)

	maximum	minimum	μ	σ
GINA 30″×30″	2816	-1541	409.85	621.74
SRTM 3″×3″	2915	0	503.47	498.98

3. COMPUTATION OF PURE GRAVIMETRIC QUASI-GEOID MODELS

The geoid computation was based on the remove-restore technique. The contribution of a geopotential model as well as the contribution of the terrain effects was subtracted from the original data. Both contributions were restored at the output. In this manner, both low and high frequencies were blocked and data with a-kind-of normal distribution were obtained. The residual geoid solution was obtained using least squares collocation in conjunction with the construction of a Residual Terrain Model (RTM) for the terrain effect estimation. The available gravity data were reduced for the effect of the global geopotential model EGM96 (Lemoine et al, 1998) (Δg_{EGM96}) and terrain effects (Δg_{RTM}) using the formula:

$$\Delta g_{red} = \Delta g_{FA} - \Delta g_{EGM96} - 2\pi G\rho(H - H_{ref}) + c \qquad (4)$$

where Δg_{FA} are the observed free-air gravity anomalies, G is Newton's gravitational constant, ρ is the mean density of the upper crust (2.67 gr/cm^3), H is the orthometric height of the computation point, H_{ref} is a reference height field representing the mean altitude of the area under consideration and c is the classical terrain correction, see e.g. Forsberg (1984). Using the reduced gravity anomalies, an empirical covariance function was computed. The analytical model used for the covariance function tabulation was the fourth model of Tscherning and Rapp (1974)

$$\sigma_i(\Delta g, \Delta g) = \frac{A(i-1)}{(i-2)(i+B)}, \tag{5}$$

where A is a free parameter to be determined and B takes the value 4. We used the error degree variances of the EGM96 geopotential model up to degree 360 and the Tscherning and Rapp model for higher degrees, according to the equation:

$$C_{\Delta g,\Delta g}(P,Q) = a\sum_{i=2}^{360} \tilde{\sigma}_i \left(\frac{R_B^2}{rr'}\right)^{i+2} P_i(\cos\psi_{PQ}) + \sum_{i=361}^{\infty} \frac{A(i-1)}{(i-2)(i+B)} \left(\frac{R_B^2}{rr'}\right)^{i+2} P_i(\cos\psi_{PQ}) \tag{6}$$

where r, r' are the distances of the points P and Q from the Earth's center, $\tilde{\sigma}_i$ the error anomaly degree variances associated with the EGM96 coefficients, a is a scale factor, R_B is the radius of the Bjerhammar sphere, P_i is the Legendre polynomials of degree i, ψ_{PQ} is the spherical distance between P and Q and A is the free parameter to be determined. An extended presentation of the covariance function estimation procedure is presented in Knudsen (1987). The final solution based on least squares collocation is (Moritz, 1980):

$$\zeta_{\Delta g} = C_{\zeta\Delta g} C_{\Delta g\Delta g}^{-1} \Delta g \tag{7}$$

Using the RTM method for the terrain effects computation a quasi-geoid is estimated. The final quasi-geoid computation is obtained using the formula:

$$\zeta = \zeta_{EGM96} + \zeta_{\Delta g} + \zeta_{RTM} \tag{8}$$

The quasi-geoid to geoid conversion can be done using (Heiskenen and Moritz, 1967):

$$\Delta\zeta = N - \zeta = \frac{\bar{g} - \bar{\gamma}}{\bar{\gamma}} H \approx \frac{\Delta g_B}{\gamma} H, \tag{9}$$

where $\bar{g}$ is the mean gravity along the plumb line, $\bar{\gamma}$ is the mean normal gravity along the normal to the ellipsoid and Δg_B is the Bouguer anomaly at the computation point. In this manner, the comparison between geoid heights from GPS/leveling and gravimetry can be done explicitly.

Table 3 summarizes the statistics of the reduced gravity data values according to each DTM type for the area of interest. It should be noted that the values for model B (SRTM) are for land only, whereas the values for model A also contain bathymetry data. The negative values represent gravity data in land areas that can be effectively reduced using dense topographic data, whereas positive data usually refers to sea areas and cannot be reduced without bathymetric data.

Table 3: Statistics of the reduced gravity values for GINA and SRTM DTMs (mGal)

	maximum	minimum	μ	σ
A - $\Delta g_{red(GINA)}$	66.215	-53.075	5.953	15.512
B - $\Delta g_{red(SRTM)}$	182.374	-58.432	5.780	19.807

The quasi-geoid solution estimated in this manner using each of the DTM is shown in Table 4. It should be noted that model A includes the residual terrain model effects of land and bathymetry as these values are available in the GINA DTM, whereas model B only contains the effects on land (as per the restrictions of the SRTM DTM).

Table 4: Pure gravimetric quasi-geoid solution based on GINA and SRTM DTMs (meters)

MODEL	maximum	minimum	μ	σ
A - $\zeta_{(GINA)}$	46.07	37.02	43.06	1.80
B - $\zeta_{(SRTM)}$	46.88	36.82	43.15	1.91

In order to investigate the quality of the pure gravimetric quasi-geoid solution we used the 132 benchmarks from GPS/leveling in the area (see section 2.3). The ellipsoidal minus orthometric geoid heights of the GPS/leveling points were transformed to quasi-geoid values in order to be directly comparable with the gravimetric solution. The statistics of the differences between pure gravimetric and GPS/leveling quasi-geoid at the control points before and after the application of a simple 4-parameter model (see Heiskanen and Moritz, 1967) are presented in Table 5 for models A and B.

Table 5: Statistics of differences between pure gravimetric quasi-geiod models (A and B) and GPS/leveling data before and after a 4-parameter bias and tilt model application (meters)

	maximum	minimum	μ	σ
MODEL A - GPS/leveling				
before fit	-2.05	-3.01	-2.40	0.25
after fit	-0.36	0.36	0.00	0.12
MODEL B – GPS/leveling				
before fit	-2.12	-2.94	-2.40	0.21
after fit	-0.37	0.34	0.00	0.12

As it seen, although the absence of the bathymetry, the high resolution of the terrain information led to best results in terms of standard deviation of the differences before bias and tilt fit. This is reasonable according to the morphology of the area: quasi-geoid computation is bounded in land area and only some minor sea parts were used in the estimation. In addition, GPS/leveling points are located in the continental part of the area under study.

4. COMPUTATION OF COMBINED GEOID MODEL SOLUTION

In order to incorporate some of the available GPS/leveling data into the computation of the geoid model, a combined solution was computed wherein gravity and GPS/leveling (and DTM) data are essentially used in a combined adjustment to compute the final geoid model. These solutions are termed Models C and D in Figure 1 and the procedure is provided herein.

We will suppose that our observations y_i may be expressed as

$$y_i = L_i(T) + e_i + A_i^T x \tag{10}$$

where L_i is a linear functional, e_i is the error, A_i a vector of partial derivatives and x the vector of parameters, see (Tscherning, 1994, section 2). If the unknown parameter is equal to N_o then A_i = 1 for all values of i which are associated with height anomalies and 0.3 mgal/m for gravity anomalies. If no parameters are present we obtain a LSC approximation to T by requiring the square of the norm of the model plus the variance of the noise to be minimized. When parameters are present we also require the square of the norm of the parameter vector to be minimized.

The covariance between two quantities will be denoted COV(L_i, L_j)= C_{ij}. If one of the functionals are the evaluation of T in a point P, we write COV(P, L_i)=C_{Pi}. The norm of a functional is denoted σ_L^2= COV (L, L), the variance-covariance of the noise σ_{ij} and $\overline{C} = \{COV(L_i, L_j) + \sigma_{ij}\}$, a n×n matrix, where n is the number of observations. Then an estimate of T and of the parameters x are obtained as

$$\begin{aligned} \tilde{T}(P) &= \{C_{Pi}\}^T \overline{C}^{-1}(y - A^T x) \\ \tilde{x} &= (A^T \overline{C}^{-1} A + W)^{-1}(A^T \overline{C}^{-1} y) \end{aligned} \tag{11}$$

where W is the a-priori weight matrix for the parameters (generally the zero matrix). The associated error estimates are with

$$H = \{COV(L, L_i)\}^T \overline{C}^{-1} \tag{12}$$

the mean square error of the parameter vector

$$m_x^2 = (A^T \overline{C}^{-1} A + W)^{-1} \tag{13}$$

and the mean square error of an estimated quantity $L(\tilde{T})$

$$m_L^2 = \sigma_L^2 - H\{COV(L, L_i)\} + HAm_x^2 (HA)^T \tag{14}$$

The statistics of the final combined quasi-geoid model solutions using each of the DTMs are provided in Table 6.

Table 6: Combined quasi-geoid solution based on GINA and SRTM DTMs (metres)

MODEL	maximum	minimum	μ	σ
C - $\zeta_{(GINA)}$	44.24	32.65	40.44	2.40
D - $\zeta_{(SRTM)}$	44.45	32.57	40.49	2.41

The comparison of the final combined quasi-geoid with the included in the solution GPS/benchmarks presents an impression of the internal accuracy of the solution. An independent control can be done using GPS measurements not included in the collocation procedure. The internal as well as the external-independent accuracy is given in Table 7.

Table 7: Accuracy assessment of the combined quasi-geoid solutions (Models C and D)

	maximum	minimum	μ	σ
MODEL C – GINA DTM				
internal (132 points)	0.23	-0.17	0.00	0.06
external (9 points)	0.21	-0.12	0.04	0.11
MODEL D – SRTM DTM				
internal (132 points)	0.23	-0.17	0.00	0.06
external (9 points)	0.21	-0.12	0.03	0.11

Considering Table 7, more than minor improvement can be identified using the dense SRTM DTM. This fact reveals the major effect of the GPS/leveling data to the combined solution. The internal as well as the external accuracy is better that the pure gravimetric solution in both DTM cases, indicating the necessity of reliable GPS measurements for combination schemes in geoid solutions. The final combined quasi-geoid solution based on GINA and SRTM DTMs are depicted in Figure 4.

4. CONCLUDING REMARKS AND FUTURE WORK

Given the overall good performance of the combined geoid model solution, as described in section 4 and validated through the analysis of results in the provided tables and figures, it is recommended that this procedure be used for computing a geoid model to be used for engineering surveys and heighting via GPS. Also, even though the density of the SRTM DTM is notably better then that of the GINA model it is recommended that GINA be employed for local geoid model computations as it contains the bathymetric data which is important for the area of interest. This is also supported by the results which do not show significant differences between models (either purely gravimetric or combined solutions) computed using GINA versus SRTM. This however could only be verified on land where the extents of both DTMs overlapped.

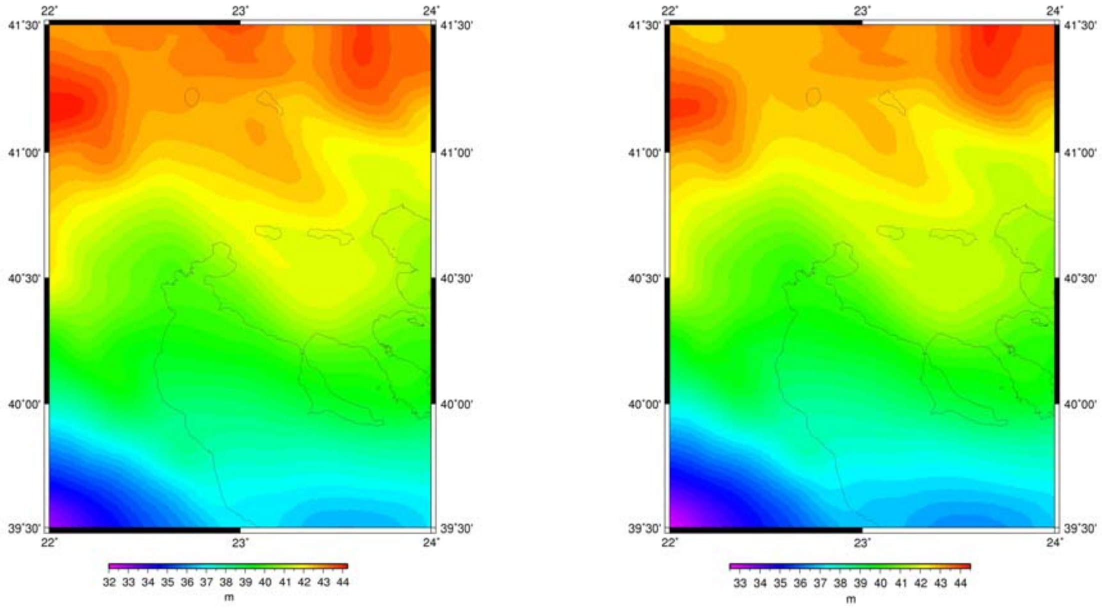

Figure 4: Final combined quasi-geoid solutions model C (left) and model D (right)

The main area for future work will concentrate on improving the quality, and equally as important, the distribution of GPS/leveling benchmark stations in northern Greece. The densely sampled areas where clusters of 35 GPS/leveling points are located (cluster a: φ = 41°, λ = 22.8°) and more than 40 points (cluster b: φ = 40.6°, λ = 22.9°) are clearly noticeable from Figure 3 and highlighted in Figure 5 below. In Figure 5 areas where there are very few (if any) benchmarks are identified. It is recommended that two measurement campaigns be launched in order to fill these gaps. The first phase will densify the more or less urban area surrounding Thessaloniki, which already contains 64% of the GPS/leveling stations. The second phase proposes the establishment of at least one station for each 0.25° × 0.5° block essentially creating a more homogenized grid of stations in the greater Thessaloniki area. Given the existing (and proposed) densified network of quality GPS/leveling points and the combined geoid solution scheme described herein, an improved geoid model can be computed.

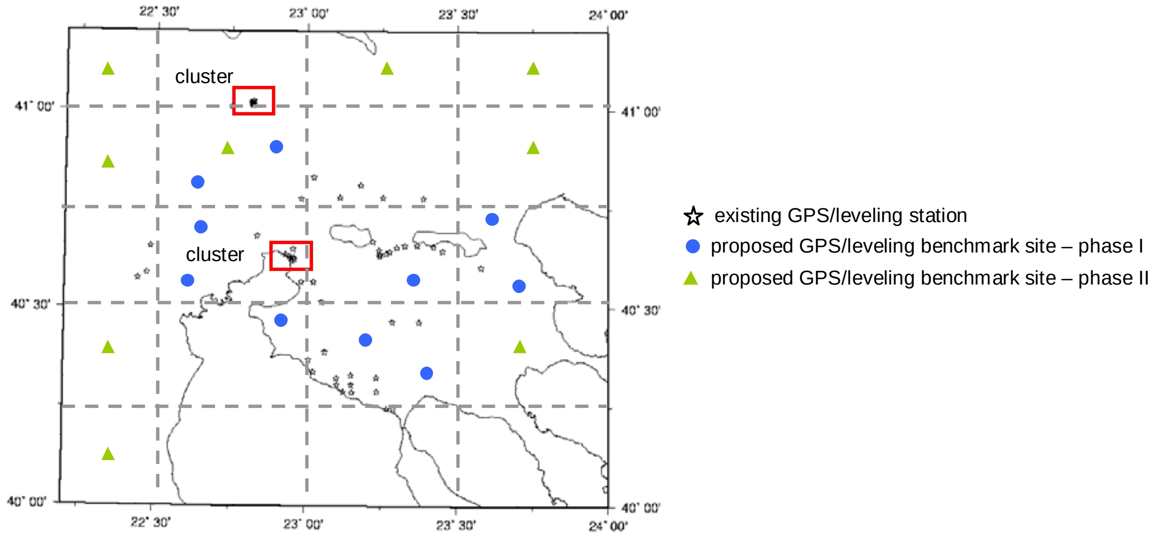

Figure 5: Proposed future sites for GPS/leveling network densification campaigns

REFERENCES

Andritsanos, V. D., Fotiou A., Kagiadakis, V., Kostakis, G., Milona-kotrogianni, E., Pikridas C., Rossikopoulos, D., and Tziavos I.N. (1999): Local Geoid Determination Combining GPS, Gravity and Height Data-A case study in the Area of Thessaloniki, Tech. Chron. Sci. J. TCG, I,3, 61-74.

Andritsanos, V. D., Fotiou A., Paschalaki E., Pikridas C., Rossikopoulos D., and Tziavos, I.N., (2000):Local Geoid Computation and Evaluation, Physics and Chemistry of the Earth, 1, 63-69.

Andersen OB, Knudsen P (1998): Global gravity field from ERS1 and Geosat geodetic mission altimetry. J Geophys Res 103(C4): 8129-8137.

BGI (1992) Bulletin d' Information, no 70, 71

Behrent, D., H. Denker, and K. Schmidt. (1996): Digital gravity data sets for the Mediterranean Sea derived from available maps. Bulletin d' information, No 78, pp. 31-39, BGI.

Forsberg (1984): A study of terrain reductions, density anomalies, and geophysical inversion methods in gravity field modeling. OSU report no 355, The Ohio State University, Columbus, Ohio.

Fotiou, A. and Pikridas C. (2002): The Global Positioning System-GPS, Lecture Notes, Aristotle University of Thessaloniki, Greece.

GINA, 2004: Internet resources: http://www.gina.alaska.edu/

Knudsen, P. (1987): Estimation and modeling of the local empirical covariance function using gravity and satellite altimetry data, Bull. Geod.,61, 145-160.

Heiskanen, W.A. and H. Moritz (1967): Physical Geodesy, W.H. Freeman and Co., San Fransisco.

Lagios E, Chailas S, Hipkin RG (1996) Newly compiled gravity and topographic data banks of Greece. Geophys J Int, 126, pp. 287 – 290.
Lemoine, F.G., S.C. Kenyon, J.K. Factor, R.G. Trimmer, N.K. Pavlis, D.S. Chinn, C.M. Cox, S.M. Klosko, S.B. Luthcke, M.H. Torrence, Y.M. Wang, R.G. Williamson, E.C. Pavlis, R.H. Rapp, and T.R. Olson (1998): The Development of the Joint NASA GSFC and the National Imagery and Mapping Agency (NIMA) Geopotential Model EGM96, NASA/TP-1998-206861, Goddard Space Flight Center, Greenbelt, MD, July.
Moritz, H.(1980): Advanced Physical Geodesy. H.Wichmann Verlag, Karlsruhe.
Pikridas, C., Andritsanos, V.D., Fotiou, A., Rossikopoulos, D., and Tziavos, I.N. (2002): Computing orthometric heights and controlling their quality by GPS and local geoid in Northern Greece. Proceedings of the 2nd European Navigation Conference GNSS, May 27-30, Copenhagen, Denmark.
Rossikopoulos, D., *Surveying networks and computations*, Aristotle University of Thessaloniki, Greece, 1999.
Rothacher and Mervart, *Bernese GPS software version 4.0*, Astronomical Institute, University of Bern, 1996.
SRTM, 2003: Internet resources: http://www.jpl.nasa.gov/srtm
Tziavos, I. N., and Andritsanos, V.D.(1999): Recent geoid computations for the Hellenic Area, Physics and Chemistry of the Earth, 24, 91-96.
Tscherning CC (1991) The use of optimal estimation for gross-error detection in databases of spatially correlated data. *BGI*, Bulletin d' Information, no 68, pp. 79 – 89.
Tscherning, C.C.(1994): Geoid determination by least-squares collocation using GRAVSOFT. Lecture Notes "Int. School of the Determination and Use of the Geoid", Milano, Oct., pp. 135 - 164, published by International Geoid Service.
Wessel, P. and Smith, W. H. F.(1995): *New version of generic mapping tools released*, EOS Trans. Amer. Geophys. U.,76, 329.

BIOGRAPHICAL NOTES

Vassilios Andritsanos: Research accosiate, Department of Geodesy and Surveying, Aristotle University of Thessaloniki. Main interests: Gravity field modelling, satellite altimetry, spectral and stochastic methods in geodesy, GPS levelling, hydrography, oceanography.

Georgia Fotopoulos: Alberta Ingenuity Fellowship (AIF) Post-Doctoral Fellow. Research interests include optimal combination of heterogeneous height data, regional geoid modelling and calibration of error models, height datums, sea level change monitoring, precise positioning and navigation, networks of GPS reference stations, RTK, WADGPS.

Aristidis Fotiou: Professor, Department of Geodesy and Surveying, Aristotle University of Thessaloniki. He expertise in adjustment theory, geometric geodesy, geodetic networks and in high precision GPS applications

Christos Pikridas: Lecturer, Department of Geodesy and Surveying, Aristotle University of Thessaloniki. His main interests are on GPS error analysis, data processing, engineering applications and deformation studies.

Dimitrios Rossikopoulos: Professor, Department of Geodesy and Surveying, Aristotle University of Thessaloniki.

Ilias Tziavos: Professor, Department of Geodesy and Surveying, Aristotle University of Thessaloniki. Main interests: Physical Geodesy, gravity field modelling, satellite altimetry, spectral and stochastic methods in geodesy, GPS and height systems, hydrography.

CONTACTS

Vasilios Andritsanos
Aristotle University of Thessaloniki
Univ. Box 440,
54124 Thessaloniki
GREECE
Tel. + 30 2310 996125
Fax + 30 2310 994859
Email: vdandrit@olimpia.topo.auth.gr

Georgia Fotopoulos
University of Calgary, Department of Geomatics Engineering
2500 University Dr NW
Calgary, AB, T2N1N4
CANADA
Tel. + 1 403 220 7106
Fax + 1 403 284 1980
Email: gfotopou@ucalgary.ca

Aristidis Fotiou
Aristotle University of Thessaloniki
Univ. Box 473,
54124 Thessaloniki
GREECE
Tel. + 30 2310 996135
Fax + 30 2310 996408
Email: afotiou@topo.auth.gr

Christos Pikridas. Lecturer
Aristotle University of Thessaloniki
Univ. Box 432,
54124 Thessaloniki
GREECE
Tel. + 30 2310 996110
Fax + 30 2310 996408
Email: cpik@topo.auth.gr
Web site: http://users.auth.gr/~kvek/cvPIK.html

Dimitrios Rossikopoulos
Aristotle University of Thessaloniki
Univ. Box 473,
54124 Thessaloniki
GREECE
Tel. + 30 2310 996115
Fax + 30 2310 996408
Email: rossi@topo.auth.gr

Ilias N. Tziavos
Aristotle University of Thessaloniki
Univ.Box 440,
54124 Thessaloniki
GREECE
Tel. + 30 2310 996125
Fax + 30 2310 995948
Email: tziavos@olimpia.topo.auth.gr
Web site: http://olimpia.topo.auth.gr